Environ Sci Pollut Res (2016) 23:18809–18822
DOI 10.1007/s11356-016-7025-2

RESEARCH ARTICLE

Spatio-temporal variation in chemical characteristics of PM_{10} over Indo Gangetic Plain of India

S. K. Sharma[1] · **T. K. Mandal**[1] · **M. K. Srivastava**[2] · **A. Chatterjee**[3] · **Srishti Jain**[1] · **M. Saxena**[1] · **B. P. Singh**[2] · **Saraswati**[1] · **A. Sharma**[1] · **A. Adak**[3] · **S. K.Ghosh**[3]

Received: 7 January 2016 / Accepted: 30 May 2016 / Published online: 18 June 2016

Abstract The paper presents the spatio-temporal variation of chemical compositions (organic carbon (OC), elemental carbon (EC), and water-soluble inorganic ionic components (WSIC)) of particulate matter (PM_{10}) over three locations (Delhi, Varanasi, and Kolkata) of Indo Gangetic Plain (IGP) of India for the year 2011. The observational sites are chosen to represent the characteristics of upper (Delhi), middle (Varanasi), and lower (Kolkata) IGP regions as converse to earlier single-station observation. Average mass concentration of PM_{10} was observed higher in the middle IGP (Varanasi $206.2 \pm 77.4\ \mu g\ m^{-3}$) as compared to upper IGP (Delhi $202.3 \pm 74.3\ \mu g\ m^{-3}$) and lower IGP (Kolkata $171.5 \pm 38.5\ \mu g\ m^{-3}$). Large variation in OC values from $23.57\ \mu g\ m^{-3}$ (Delhi) to $12.74\ \mu g\ m^{-3}$ (Kolkata) indicating role of formation of secondary aerosols, whereas EC have not shown much variation with maximum concentration over Delhi ($10.07\ \mu g\ m^{-3}$) and minimum over Varanasi ($7.72\ \mu g\ m^{-3}$). As expected, a strong seasonal variation was observed in the mass concentration of PM_{10} as well as in its chemical composition over the three locations. Principal component analysis (PCA) identifies the contribution of secondary aerosol, biomass burning, fossil fuel combustion, vehicular emission, and sea salt to PM_{10} mass concentration at the observational sites of IGP, India. Backward trajectory analysis indicated the influence of continental type aerosols being transported from the Bay of Bengal, Pakistan, Afghanistan, Rajasthan, Gujarat, and surrounding areas to IGP region.

Keywords PM_{10} · Organic carbon · Elemental carbon · Water-soluble ions · IGP

Introduction

The Indo Gangetic Plain (IGP) is the major source of pollutants over India and Indian subcontinents due to the combined effect of the usage of fossil fuels and biomass fuels as energy, rapid urbanization, and industrialization (Tare et al. 2006; Ram and Sarin 2011; Saud et al. 2013; Sharma et al. 2014a, b, c). It is well documented that atmospheric particulate matter (PM) significantly affects atmospheric chemistry, ambient air quality, visibility, climate change, cloud formation, and the Earth's radiation budget (Ramgolam et al. 2009; Pope et al. 2009). Several studies have revealed that aerosols can lead to serious human health effects like cardiovascular and respiratory disorders (Pope and Dockery 2006). Generally, coarse mode PM are natural while fine-mode PM are produced due to chemical conversion such as the gas to particle conversion, combustion of fuels in vehicles, or high industrial processes (Sharma et al. 2015; Perrino et al. 2011). Therefore, chemical characterization and identification of PM sources are necessary to develop air quality improvement strategies in order to be able to control and reduce ambient PM concentrations through targeted action (Waked et al. 2014).

Responsible editor: Gerhard Lammel

Electronic supplementary material The online version of this article (doi:10.1007/s11356-016-7025-2) contains supplementary material, which is available to authorized users.

✉ S. K. Sharma
sudhir.npl@nic.in; sudhircsir@gmail.com

[1] Radio and Atmospheric Sciences Division, CSIR-National Physical Laboratory, Dr. K S Krishnan Road, New Delhi 110 012, India

[2] Department of Geophysics, Banaras Hindu University, Varanasi 221 005, India

[3] Centre for Astroparticle Physics and Space Sciences, Bose Institute, Kolkata 700091, India

Particulate matter has been extensively studied in recent years over the continents including IGP region due to its potential impacts on human health and air quality (Schwartz et al. 1996; Li et al. 2009; Ram et al. 2012; Sharma et al. 1995; Sharma et al. 2014a, b; Sen et al. 2014). The previous studies (Ram and Sarin 2010; Ram et al. 2012; Sharma et al. 2014a, b) demonstrated that the soil dust, agricultural activities, biomass burning, vehicular emission, and industries, are responsible for the formation of secondary inorganic particles and other anthropogenic sources over IGP, India. Most of the studies on chemical characteristics of aerosol over IGP region are reported based on single location experiment/observation; long-term and simultaneous observations of chemical properties of PM over several locations of IGP are limited. The variation in inorganic secondary particle is of greater significance from the human health point of view and need to be examined (Liousse et al. 1996; Jacobson 2001; Sharma et al. 2007; Li et al. 2009; Bond et al. 2013).

Earlier studies have concentrated at a particular location only, rather representing regional features of whole IGP region. Present study documents the spatial and temporal variability of chemical composition of ambient aerosols through ground-based measurements over the whole IGP region. Keeping in view of the competitive importance and sensitivity of role of seasonal wind flow patterns, and production from local sources, chemical properties of aerosol over IGP, India, have also been discussed. The paper represents the simultaneous sampling of PM_{10} mass and analysis of chemical compositions (organic carbon (OC), elemental carbon (EC), and water-soluble inorganic ionic component (WSIC)) over three sites of IGP, India, (Delhi, Varanasi, and Kolkata) stretching from upper IGP region to lower IGP region for the whole year of 2011.

Methodology

Sites description

The observational sites are chosen to represent the characteristics of upper (Delhi), middle (Varanasi), and lower (Kolkata) IGP region of India. Saud et al. (2011, 2013) represent that IGP as a whole is a major emitter of pollutants, although emission density varies from spatially over IGP region. Therefore, three sites may represent the combination of local sources as well as the transported features of particulate matter. The description of the study sites are as follows: PM_{10} samples were collected at CSIR-National Physical Laboratory (28° 38′ N, 77° 10′ E; 218 m amsl), New Delhi, India (Fig. 1). The sampling site represents a typical urban atmosphere, surrounded by huge roadside traffic and agricultural fields in the southwest direction. During 2010–2011, the total number of registered vehicles in Delhi were approximately 6.35 million (Delhi Statistical Handbook 2012). This area is under the influence of free airmass flow from northeast to northwest in winter and from southeast to southwest in the summer (Goyal and Sidhartha 2002; Sharma et al. 2014a). During winter, Delhi experiences severe fog and haze weather conditions and poor visibility. During summer, the occasional occurrence of dust storm contributes the presence of mineral dust significantly to the aerosol loading (Ram et al. 2010). The ambient temperature of sampling site of Delhi varies from minimum (1 °C) in winter (November to February) to maximum (48 °C) in summer (March to June). During monsoon (July to October), the average rainfall at the sampling site is recorded as 780 mm.

The sampling site, Varanasi (25° 18′ N, 83° 03′ E; 129 m amsl) located in the middle Ganges valley of North India (Fig. 1) represent an urban environment. Being located in the IGP of North India, the land is very fertile due to low-level floods in the Ganges continually replenishing the soil. Varanasi experiences a humid subtropical climate with large variations between summer and winter temperatures. The temperature of the sampling site ranges between 22 and 46 °C in the summer. During winter, Varanasi faces very large diurnal variations with warm days and downright cold nights. Cold waves from the Himalayan region cause temperatures to dip across the city in the winter from December to February, and temperature below 5 °C is common. The average annual rainfall is recorded as 1110 mm during 2011.

The sampling site, Kolkata, a megacity (22° 33′ N and 88° 20′ E; 9 m amsl), represents a typical urban environment located in the lower IGP influenced by upwind aerosol. The site is bounded to the west and northwest by Houghly river spread along 80 km. Sundarban mangroves forest, the world's largest mangrove eco-region at the land-ocean boundary of the Ganges delta, is situated about 100 km from Kolkata. The average temperature, RH, and wind speed of the sampling site during study recorded as 23 °C, 74 %, and 2.1 m s^{-1}, respectively.

Aerosol sampling

PM_{10} samples were collected (4–5 samples/month) at Delhi (n = 50), Varanasi (n = 45), and Kolkata (n = 54) of IGP, India, on precombusted (at 550 °C for 5 h to eradicate organic impurities and kept in desiccators for 24 h prior to sample collection) Whatman Quartz Microfibre filters (QM-A) at a 10-m height (AGL) during January to December 2011. Particle samplers (model: PEM-RDS 8NL, Make: M/s. Polltech Instruments, Mumbai, India) were used to collect the PM_{10} samples at all the locations. The blower flow rates of the samplers were calibrated (with the accuracy of ±1 % of full scale) with top loading orifice calibrator traceable to national standard. The flow meters of the samplers were also calibrated (with the accuracy of ±2 %

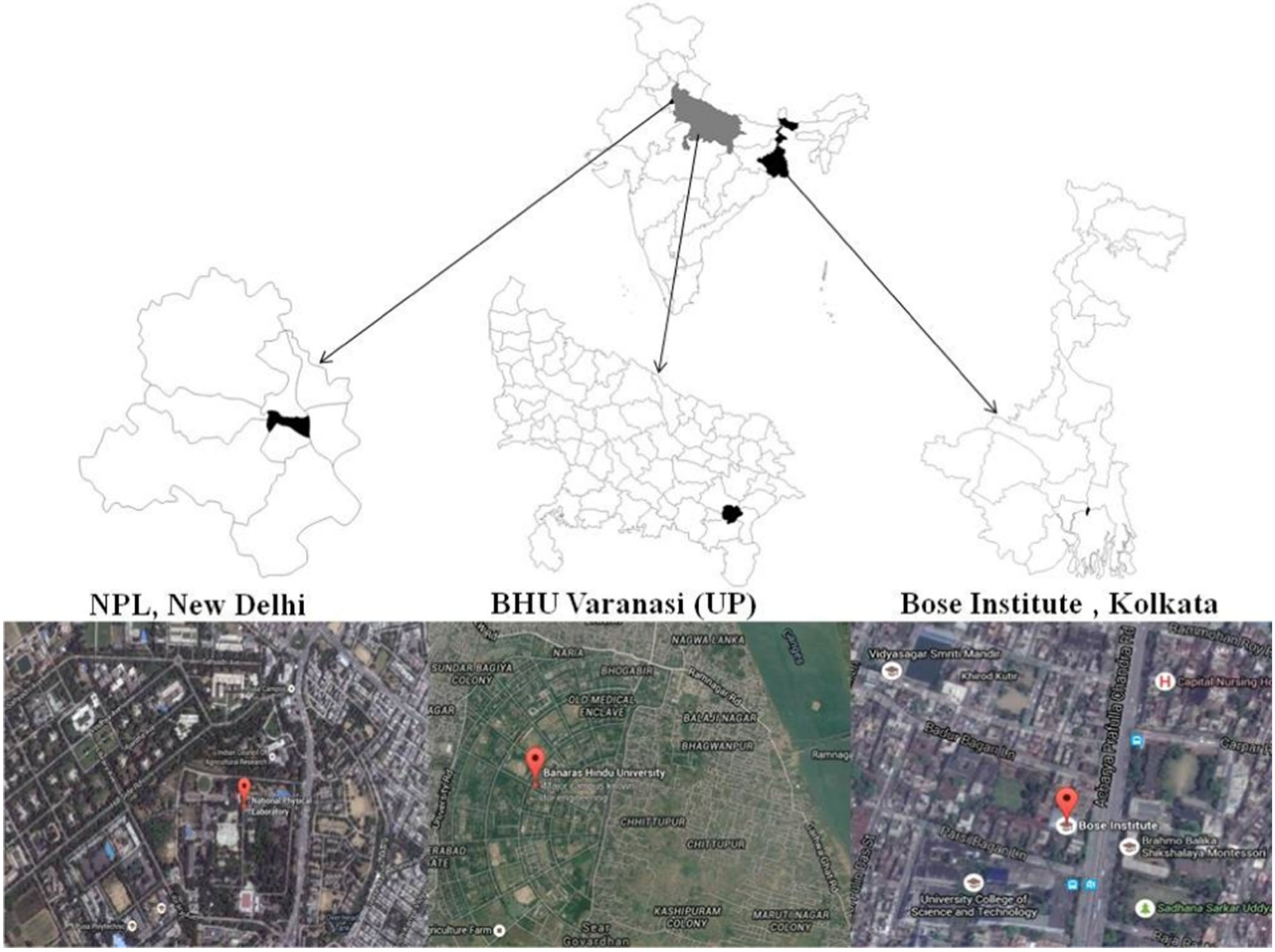

Fig. 1 Map of observational sites (Delhi, Varanasi, and Kolkata), IGP, India

of full scale) with air flow calibrator traceable to national standard. Ambient air was passed through QM-A filters (size 20 × 25 cm^2) at a flow rate of 1.13 m^3 min^{-1} (accuracy ±2 %) for 8 h on a day and night basis [during the daytime (1000–1800 h) and nighttime (1900–0300 h)]. In general, rush hour started from 0900 to 1100 hours and 1700 to 1900 hours in Delhi (Sharma et al. 2010); hence, the sampling had been started at 1000 hours (at daytime) and 1900 hours (at nighttime). The sample has been collected for 8 h also to follow the common protocol (i.e., 8 or 12 or 24 h) of Central Pollution Control Board (CPCB), New Delhi, India. The average concentration of day and night sampling of PM$_{10}$ was reported in the paper. The sample filters were weighed before and after the sampling during the experiment in order to determine the mass of the PM$_{10}$ collected. The concentration of PM$_{10}$ (μg m^{-3}) was calculated on the basis of the difference between final and initial weights of the QM-A filters (measured by a microbalance; resolution ±10 μg) and divided by the total volume of air passed during the sampling. After collecting samples, filters were stored under dry condition at −20 °C in deep-freezer prior to analysis.

Analysis

OC and EC analysis

Analysis of OC and EC of ambient PM$_{10}$ samples was performed using an OC/EC carbon analyzer (model: DRI 2001 A, Atmoslytic Inc., Calabasas, CA, USA) following the USEPA Method (Improve Protocol) with negative pyrolysis areas zeroed (Chow et al. 2004). The detail principle and analytical procedure for analysis of OC and EC species of PM$_{10}$ mass are described in Chow et al. (2004). Approximately 0.536 cm^2 area of QM-A filter was cut using the proper punch, and the values are reported as μg cm^{-2} as given by the instrumental analysis software. Each filter was analyzed triplicate with blank filters (blank filters analyzed) to get the representative estimation of OC and EC concentration in PM$_{10}$. To estimate the accurate OC and EC concentrations, the OC and EC values of blank filters were estimated and subtracted from the sample filters. The analytical error (repeatability) was estimated to be 3–5 % based on triplicate analysis of each filters.

Water-soluble inorganic ionic components analysis

PM_{10} samples were extracted in deionized water having conductivity >18.2 MΩ for 90 min in ultrasonic extractor for the determination of WSIC (Na^+, NH_4^+, K^+, Ca^{2+}, Mg^{2+} F^-, Cl^-, NO_3^-, and SO_4^{2-}). The WSIC of PM_{10} has been analyzed by ion chromatograph (model: DIONEX-ICS-3000, Sunnyvale, CA, USA). The concentrations of F^-, Cl^-, NO_3^-, and SO_4^{2-} were determined by using an Ion Pac-AS11-HC analytical column with a guard column, ASRS-300 4 mm anion micro-membrane suppressor, 20 mM NaOH (50 % *w*/*w*) as eluent, and triple-distilled water as regenerator. Li^+, Na^+, NH_4^+, K^+, Ca^{2+}, and Mg^{2+} were determined by using a separation column with a guard column, suppressor CSRS-300 and 5 mM MSA (methane sulfonic acid) as eluent. Calibration standards have been prepared by the National Institute of Standards and Technology (NIST, USA) traceable certified standards for calibration of IC (Sharma et al. 2014d). The blank filters were also analyzed for cations (Li^+, Na^+, NH_4^+, K^+, Ca^{2+}, and Mg^{2+}) and anions (F^-, Cl^-, NO_3^-, and SO_4^{2-}). The analytical error (repeatability) was estimated to be 3–5 % based on triplicate analysis of each filters (Sharma et al. 2012a).

Meteorological parameters and trajectory analysis

Meteorological parameters such as temperature (accuracy ±1 °C), relative humidity (RH) (accuracy ± 2 %), wind direction (accuracy ±3°), and wind speed (accuracy ±2 % of full scale) were collected at every 5-min interval using automatic weather station (AWS) at all the sampling sites. In order to identify the possible transport pathways of PM_{10} from their potential sources of origin to Delhi, Varanasi, and Kolkata of IGP, India, 5-day backward trajectory was calculated using the Hybrid Single Particle Lagrangian Integrated Trajectory (HYSPLIT) model and has been traced (Draxler and Rolph 2003). Air mass back-trajectories for each experimental day for 500 m above the ground level (AGL) during January to December 2011 have been calculated using Global Data Assimilation System (GDAS) meteorological data. HYSPLIT was run every day starting at 0500 hours, UTC, at a starting height of 500 m AGL on an hourly basis for each site. This height was chosen to diminish the effects of surface friction and to represent winds in the low boundary layer. The PM_{10} has the ability to travel long distance; therefore, 5 days were selected to calculate backward trajectories using HYSPLIT.

Principal component analysis

Principal component analysis (PCA) was performed to identify the possible sources of PM_{10} mass over Delhi, Varanasi, and Kolkata of IGP, India. In the present study, the orthogonal transformation method with Varimax rotation was employed. The lowest Eigenvalue for extracted factors was restricted to more than 1.0. Total 11 constituents of PM_{10} were used as variable in the dataset. In PCA, the chemical data are transformed into a dimensionless standardized form:

$$Zij = \frac{Cij - \bar{C}j}{\sigma j} \tag{1}$$

where $i = 1, \ldots, n$ samples; $j = 1, \ldots m$ elements; Cij is the concentration of element j in sample i; and $\bar{C}j$ and σj are the arithmetic mean concentration and the standard deviation for element j, respectively. The PCA model is expressed as

$$\mathrm{Z_{ij}} = \sum\nolimits_{k=1}^{p} g_{ik} h_{kj} \tag{2}$$

where $k = 1, \ldots, p$ sources, and g_{ik} and h_{kj} are the factor loadings and the factor scores, respectively. This equation is solved by Eigenvector decomposition (Song et al. 2006).

Results and discussion

Mass concentration

In the previous section, we have mentioned that the observational sites are chosen to represent the characteristics of upper (Delhi), middle (Varanasi), and lower (Kolkata) IGP regions; therefore, in the following sections, we will discuss the results of individual stations. The annual average mass concentration of PM_{10} over Delhi (range 63.3–354.7 μg m^{-3}), Varanasi (range 53.3–392.1 μg m^{-3}), and Kolkata (range 92.9–382.6 μg m^{-3}) was recorded as 202.3 ± 74.3, 206.2 ± 77.4, and 171.5 ± 38.5 μg m^{-3}, respectively (Table 1), indicating the events of higher mass concentration over Varanasi as well as large variation among the three observational sites of IGP, India. Higher mass concentration of PM_{10} in the middle IGP indicates combined influences of the accumulation of fine particulates advected from the upper IGP region and local sources (transport for usage of adulterated oil, brick kiln, biomass burning, etc.). Combination of PCA analysis and trajectory analysis may provide better insight of the higher mass concentration of PM_{10} mass. The temporal variation of PM_{10} concentration over IGP region is also depicted in Fig. 2.

Figure 3 shows the monthly average (average ± SD) of mass concentrations of PM_{10}, OC, and EC over Delhi, Varanasi, and Kolkata of IGP, India, during 2011. Delhi and Varanasi have recorded almost similar order of magnitude of monthly average concentration of PM_{10} (Fig. 3) as 333.6 and 366.6 μg m^{-3}, respectively, in the month of December (winter), whereas the highest concentration of Kolkata was recorded as 244.3 μg m^{-3} in the month of January. All the three sites, viz., Delhi, Varanasi, and Kolkata, have recorded the lowest monthly average value as 101.9 μg m^{-3} (July), 69.5 μg m^{-3} (August), and 119.5 μg m^{-3} (June), respectively, during monsoon. Average

Table 1 The average concentrations of particulates (PM_{10}), EC, OC, and WSIC of PM_{10} ($\mu g\ m^{-3}$) over IGP, India

Species	Season					Seasonal difference		
	Annual	Range	Winter (W)	Summer (S)	Monsoon (M)	W-S	W-M	S-M
Delhi (winter, $n = 17$; summer, $n = 17$; monsoon, $n = 16$)								
PM_{10}	202.25 ± 74.34	63.29–354.73	263.77^{a}	209.15^{a}	133.84^{a}	54.62^{*}	129.93^{*}	75.31^{*}
OC	22.66 ± 7.39	10.40–50.01	28.55^{a}	21.21	18.20^{a}	7.34^{*}	10.45^{*}	3.01^{*}
EC	8.69 ± 3.99	1.65–29.39	11.67^{a}	8.69^{a}	5.71^{a}	2.98^{*}	5.96^{*}	2.98^{*}
Cl^{-}	4.49 ± 3.49	0.45–19.72	6.23^{a}	3.72	2.86	2.46	3.37	0.91
SO_4^{2-}	11.60 ± 3.68	3.81–24.65	13.29^{a}	12.83	8.68^{a}	0.46^{*}	4.61^{*}	4.15^{*}
NO_3^{-}	10.54 ± 5.53	0.77–32.15	16.35^{a}	9.57^{a}	5.70^{a}	6.77^{*}	10.65^{*}	3.87^{*}
NH_4^{+}	5.19 ± 4.18	0.28–19.08	9.41^{a}	3.59^{a}	2.58^{a}	5.82^{*}	6.82^{*}	1.00
Na^{+}	3.51 ± 1.86	0.87–7.81	1.86^{a}	3.20^{a}	5.45^{a}	−1.34	-3.59^{*}	-2.24^{*}
K^{+}	1.75 ± 0.74	0.52–4.67	1.78	1.37	2.09	0.41	−0.31	−0.72
Mg^{2+}	0.75 ± 0.21	0.19–1.45	0.72	0.80	0.72	−0.08	0.00	0.07
Ca^{2+}	4.75 ± 1.19	1.17–9.77	4.42	4.88	4.95	−0.45	−0.52	−0.07
Varanasi (winter, $n = 17$; summer, $n = 17$; monsoon, $n = 11$)								
PM_{10}	206.17 ± 77.44	53.32–392.07	290.49	177.87^{a}	148.14^{a}	110.62^{*}	142.34^{*}	31.73^{*}
OC	16.93 ± 8.64	5.85–51.90	24.94^{a}	12.51	13.33^{a}	12.42^{*}	11.61^{**}	-0.82^{*}
EC	7.31 ± 5.14	0.99–28.75	12.41^{a}	4.48^{a}	5.03^{a}	7.93^{*}	7.38^{*}	-0.56^{*}
Cl^{-}	5.84 ± 4.63	0.69–17.83	9.62^{a}	2.93	4.96	6.69	4.66	2.03
SO_4^{2-}	10.71 ± 6.04	1.66–25.19	16.74^{a}	5.38^{a}	9.99^{a}	11.35^{*}	6.74^{*}	-4.61^{*}
NO_3^{-}	8.72 ± 6.55	0.81–25.78	16.66^{a}	3.62^{a}	5.88^{a}	13.04^{*}	10.78^{*}	-2.25^{*}
NH_4^{+}	3.42 ± 4.07	0.12–15.24	7.77^{a}	1.19^{a}	1.30^{a}	6.58^{*}	6.47^{*}	-0.11^{*}
Na^{+}	2.92 ± 0.94	0.50–8.81	3.78	2.69	2.29	1.10	1.50	0.40
K^{+}	1.69 ± 0.79	0.45–4.42	2.03	1.78	1.26	0.25	0.77	0.52
Mg^{2+}	0.61 ± 0.29	0.25–2.09	0.77	0.55	0.52	0.22	0.25	0.03
Ca^{2+}	3.67 ± 1.53	0.94–8.58	4.25	3.50	3.24	0.75	1.01	0.26
Kolkata (winter, $n = 15$; summer, $n = 22$; monsoon, $n = 17$)								
PM_{10}	171.48 ± 38.46	92.92–382.63	203.99^{a}	140.75^{a}	169.71^{a}	63.23^{*}	34.29^{*}	-28.95^{*}
OC	13.68 ± 5.27	5.32–55.20	18.90^{a}	10.56^{a}	11.58^{a}	8.34^{*}	7.32^{*}	-1.02^{*}
EC	7.83 ± 4.04	2.17–20.04	12.18^{a}	5.29^{a}	6.03^{a}	6.09^{*}	6.14^{*}	-0.74^{*}
Cl^{-}	9.54 ± 3.41	3.96–35.08	13.59^{a}	7.43	7.60	6.15^{*}	5.98	−0.17
SO_4^{2-}	10.04 ± 2.94	2.09–27.71	13.49^{a}	7.84^{a}	9.09^{a}	5.65^{*}	4.40^{*}	-1.25^{*}
NO_3^{-}	6.49 ± 2.68	2.12–21.44	6.97^{a}	8.21^{a}	4.43^{a}	-1.43^{*}	2.35^{*}	3.78^{*}
NH_4^{+}	6.99 ± 3.02	0.37–14.60	8.33^{a}	5.31^{a}	7.32^{a}	3.02^{*}	1.01^{*}	−2.01
Na^{+}	5.40 ± 1.34	2.06–11.66	6.09	5.34	4.78	0.76	1.32	0.56
K^{+}	3.07 ± 1.92	0.34–16.78	5.06	2.21	1.95	2.86	3.11	0.26
Mg^{2+}	0.78 ± 0.19	0.20–1.68	1.00	0.68	0.68	0.32	0.32	−0.01
Ca^{2+}	4.93 ± 2.52	1.35–19.56	7.28	3.44	3.74	3.50	3.54	0.04

[*] Significant at $P < 0.05$

[a] Significantly (intraseasonal) different at $P < 0.05$

day and night ratio of PM_{10} over Delhi, Varanasi, and Kolkata were recorded as 1.01, 1.00, and 0.94 during the study (Fig. S1; in supplementary information). Several studies on PM_{10} concentration over individual stations of IGP are reported earlier, e.g., Tiwari et al. (2012) have reported the annual average concentration of PM_{10} mass as 219 ± 84 $\mu g\ m^{-3}$ during 2007, whereas Sharma et al. (2014b) reported annual PM_{10} mass concentration as 213.1 ± 15.0 $\mu g\ m^{-3}$ over Delhi during 2010. In another study, Sharma et al. (2014a) reported annual PM_{10} concentration over Delhi to be 191.4 ± 45.5 $\mu g\ m^{-3}$ for the period 2010–2011. Pandey et al. (2013) also reported the PM_{10} mass concentrations over Lucknow during 2007 to 2009 of the order of 168.1 ± 29.1 $\mu g\ m^{-3}$ (range 102.3–240.5 $\mu g\ m^{-3}$). Murari et al. (2014) reported the annual average concentration of PM_{10} as 176.1 ± 85.0 $\mu g\ m^{-3}$ during 2013–2014 at Varanasi. Das et al. (2006) have reported

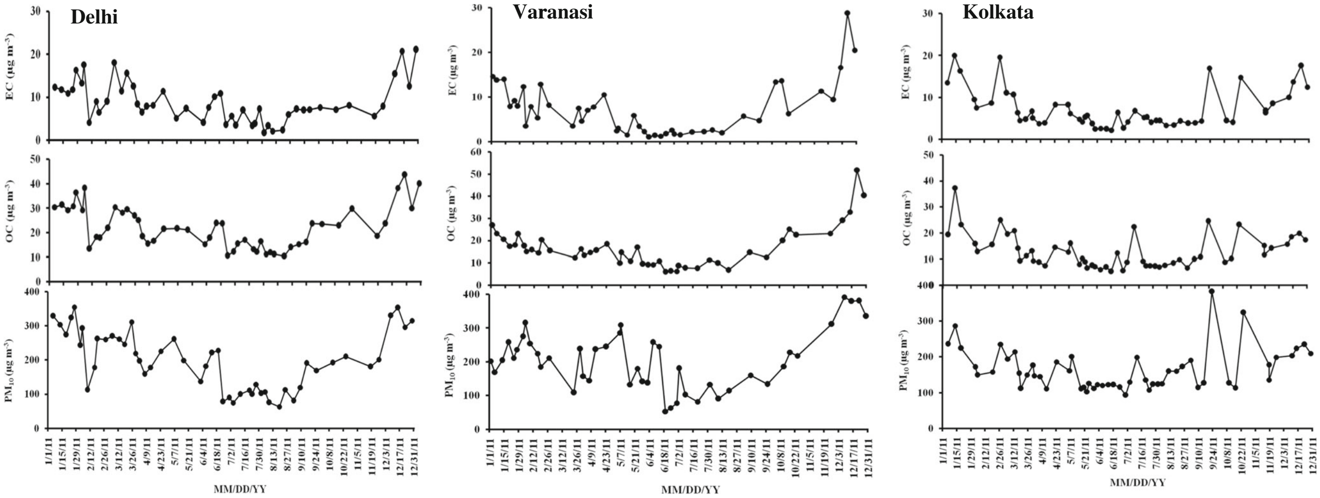

Fig. 2 Temporal variability in mass concentrations of PM_{10} and OC and EC of PM_{10} at urban sites of Delhi, Varanasi, and Kolkata

average PM_{10} mass concentration to be 303.85 ± 49.48 μg m^{-3} over Kolkata, whereas Gupta et al. (2007) reported as 288.93 ± 123.52 μg m^{-3}. The highest concentration of PM_{10} mass during the winter months over IGP may be due to the combined effect of source strength and lower boundary layer height (Datta et al. 2010; Ram and Sarin 2010; Sharma et al. 2015).

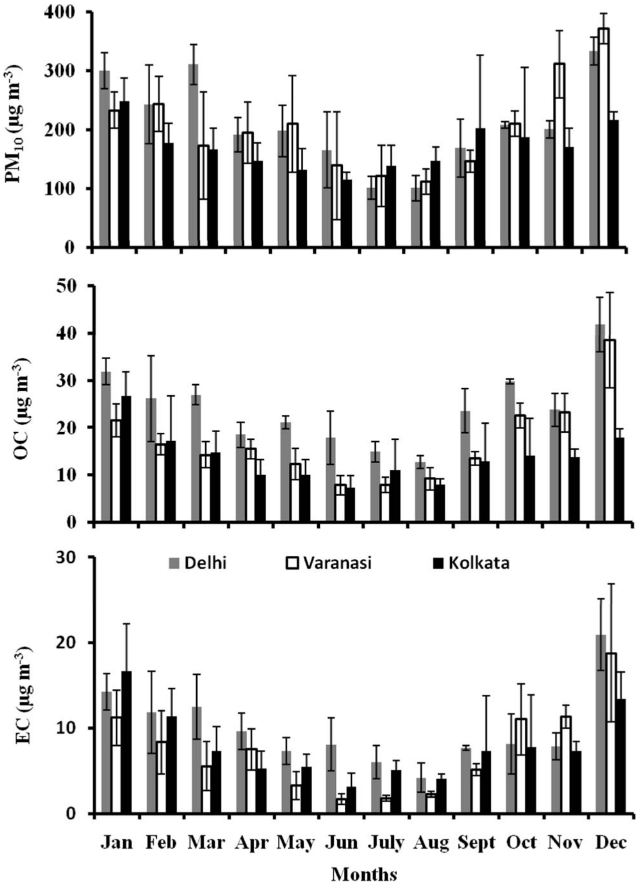

Fig. 3 Monthly average variations in mass concentration of PM_{10}, OC, and EC (μg m^{-3}) over Delhi, Varanasi, and Kolkata of IGP, India, during 2011

The mass concentration of PM_{10} during winter, summer, monsoon, and its seasonal differences over Delhi, Varanasi, and Kolkata of IGP, India, are also summarized in Table 1. The average mass concentration of PM_{10} was recorded as 263.7 μg m^{-3} (winter), 209.2 μg m^{-3} (summer), and 133.8 μg m^{-3} (monsoon) over Delhi. The higher average PM_{10} mass was recorded at all the observational sites of IGP, India, during winter, when low-level northeast wind flow carries large amount of pollutants along with as well as lower boundary layer caps pollutant increasing the average burden, whereas lower values were observed during monsoon, except Kolkata (Table 1). Large amount of sea salt might have increased the concentration of PM_{10} pouring into the atmosphere over Kolkata. This may be reconfirmed from the inorganic component of the chemical composition. In the present case, the significant seasonal variations in concentration of PM_{10} were observed at all the sites.

Chemical composition

Chemical compositions (OC, EC, and WSIC) of PM_{10} samples collected over Delhi, Varanasi, and Kolkata are summarized in Table 1 with seasonal changes. Figures 3 and 4 show the monthly average variations of mass concentrations and fractions of OC, EC, and WSIC of PM_{10} over IGP, India, during 2011. The detail descriptions of chemical characteristics of PM_{10} over the region are described in the next section.

Time series of PM_{10}, OC, and EC concentrations over Delhi, Varanasi, and Kolkata during January–December 2011 are depicted in Fig. 2. Over Delhi, the highest concentration of PM_{10} mass was recorded as 354.7 μg m^{-3} during January, whereas minimum concentration of PM_{10} mass was recorded as 63.3 μg m^{-3} during August. Over Varanasi, the highest concentration of PM_{10} mass was recorded as 392.1 μg m^{-3} during December, whereas minimum concentration of PM_{10} mass was recorded as 53.3 μg m^{-3} during June (Fig. 2). Unlike other two stations, the highest concentration

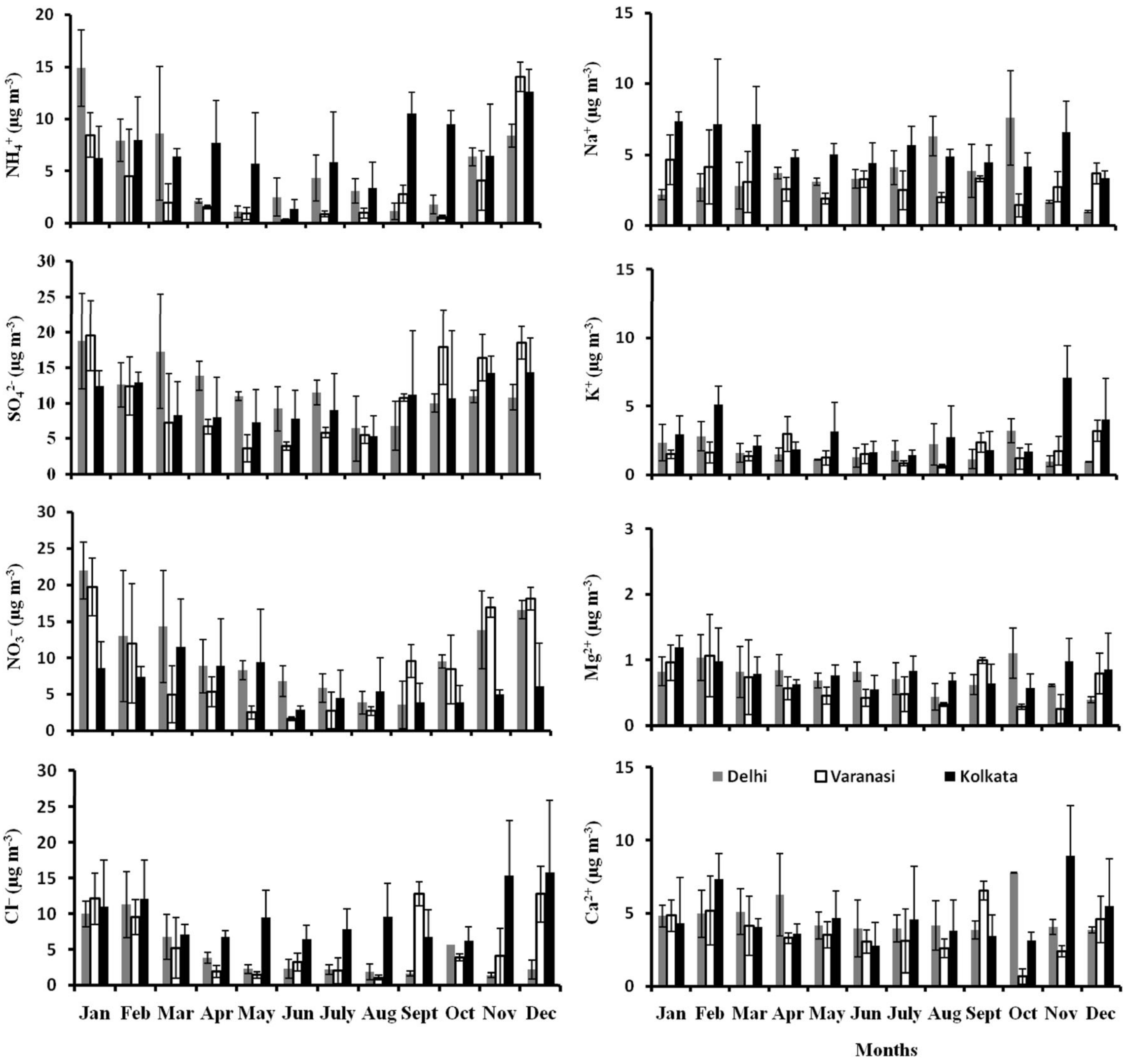

Fig. 4 Monthly average variations in mass concentration of WSIC (µg m^{-3}) of PM_{10} over Delhi, Varanasi, and Kolkata of IGP, India, during 2011

of PM_{10} mass (as 382.6 µg m^{-3}) was recorded over Kolkata during January the period of transition between monsoon and winter season. WSIC of PM_{10} also followed the similar temporal variation over the IGP region.

It has been noticed that concentration of OC, EC, and total carbon (TC = OC + EC) has followed the pattern of variation of PM_{10} mass concentration with maximum concentration broadly in winter (December–February) over the three stations. The monthly variations in chemical composition of PM_{10} at observational sites of IGP indicate that the (Figs. 3 and 4) higher average concentration of OC in PM_{10} (41.9 µg m^{-3}) was observed in the month of December in Delhi, followed by Varanasi (38.5 µg m^{-3}), whereas Kolkata recorded the highest value (25.9 µg m^{-3}) in the month of February. The EC has followed similar pattern with the maximum concentration in the month of December at Delhi (20.9 µg m^{-3}), followed by Kolkata (20.2 µg m^{-3}), whereas Varanasi has recorded the highest value (19.1 µg m^{-3}) in the month of February. It is to be reminded that total carbon (TC) content accounts for ~16 % of PM_{10} mass at Delhi during 2011 following the pattern of OC and EC with higher concentration during December (winter). During 2010, the total carbon (TC) had been accounted for ~18 % of PM_{10} mass at Delhi (Sharma et al. 2014c). Concentrations of OC, EC, and TC have varied with the increase of aerosol loading.

Organic carbon and elemental carbon

Over Delhi, annual concentration of OC has been varied from 10.4 to 50.1 µg m^{-3} with an average value of 22.7 ± 7.3 µg m^{-3} (~11 % of PM_{10} mass), whereas mass concentration of EC has varied from 1.7 to 29.4 µg m^{-3} with an average value of 8.7 ± 4.0 µg m^{-3} (~5 % of PM_{10} mass). The average concentration of OC has been recorded as 16.9 ± 8.6 µg m^{-3} (~8 % of PM_{10} mass) and 13.7 ± 5.3 µg m^{-3} (~9 % of PM_{10} mass) at Varanasi and

Kolkata, respectively, whereas average concentration of EC was observed as 7.3 ± 5.1 μg m^{-3} (~5 % of PM_{10} mass) and 7.8 ± 4.0 μg m^{-3} (~4 % of PM_{10} mass) over Varanasi and Kolkata, respectively (Table 1).

It is to be reminded that TC content accounts for ~16 % of PM_{10} mass at Delhi during 2011 following the pattern of OC and EC with higher concentration during December (winter). During 2010, the total carbon (TC) had been accounted for ~18 % of PM_{10} mass at Delhi (Sharma et al. 2014c). Ram and Sarin (2010) have reported that total carbonaceous aerosol (TCA = OM + EC) accounts for ~30–35 % of the total suspended particulate (TSP) mass at urban and rural sites of northern India (whereas in the present study, it is accounted for ~29 % of PM_{10} mass). Over an urban site (Beijing) in China, Guinot et al. (2007) have reported that 46 % of fine aerosol (<2 μm) mass is composed of carbonaceous aerosols. Recently, Mandal et al. (2014) had reported very higher annual average concentrations of OC (93.0 ± 44.7 μg m^{-3}), EC (27.3 ± 13.4 μg m^{-3}), and total carbonaceous aerosols (176.1 ± 84.7 μg m^{-3}; ~66 % of PM_{10} mass) in PM_{10} (average 280.7 ± 126.1 μg m^{-3}) mass at an industrial area of Delhi, India.

In the present case, the average day and night ratio of OC were recorded as 0.79, 0.85, and 0.90 over Delhi, Varanasi, and Kolkata, respectively, whereas the average day and night ratio of EC were recorded as 0.60, 0.73, and 0.68 at Delhi, Varanasi, and Kolkata, respectively (Fig. S1; in supplementary information). Ram and Sarin (2011) also reported the similar type of observations at Kanpur, a site in the middle IGP, India, and attributed this increment in mass concentration of PM_{10} during nighttime at the observational site to increase in the source strength of cabonaceous species and trapping of aerosols due to lowering of boundary layer height, etc. (Sharma et al. 2014b). Abundance of OC and EC concentration shows a linear increment with aerosol mass of PM_{10} at all the locations (Fig. 5).

The monthly variations in chemical composition of PM_{10} at observational sites of IGP indicate that the (Figs. 3 and 4) higher average concentration of OC in PM_{10} (41.9 μg m^{-3}) was observed in the month of December in Delhi, followed by Varanasi (38.5 μg m^{-3}), whereas, Kolkata recorded the highest value (25.9 μg m^{-3}) in the month of February. The EC has followed similar pattern with the maximum concentration in the month of December at Delhi (20.9 μg m^{-3}), followed by

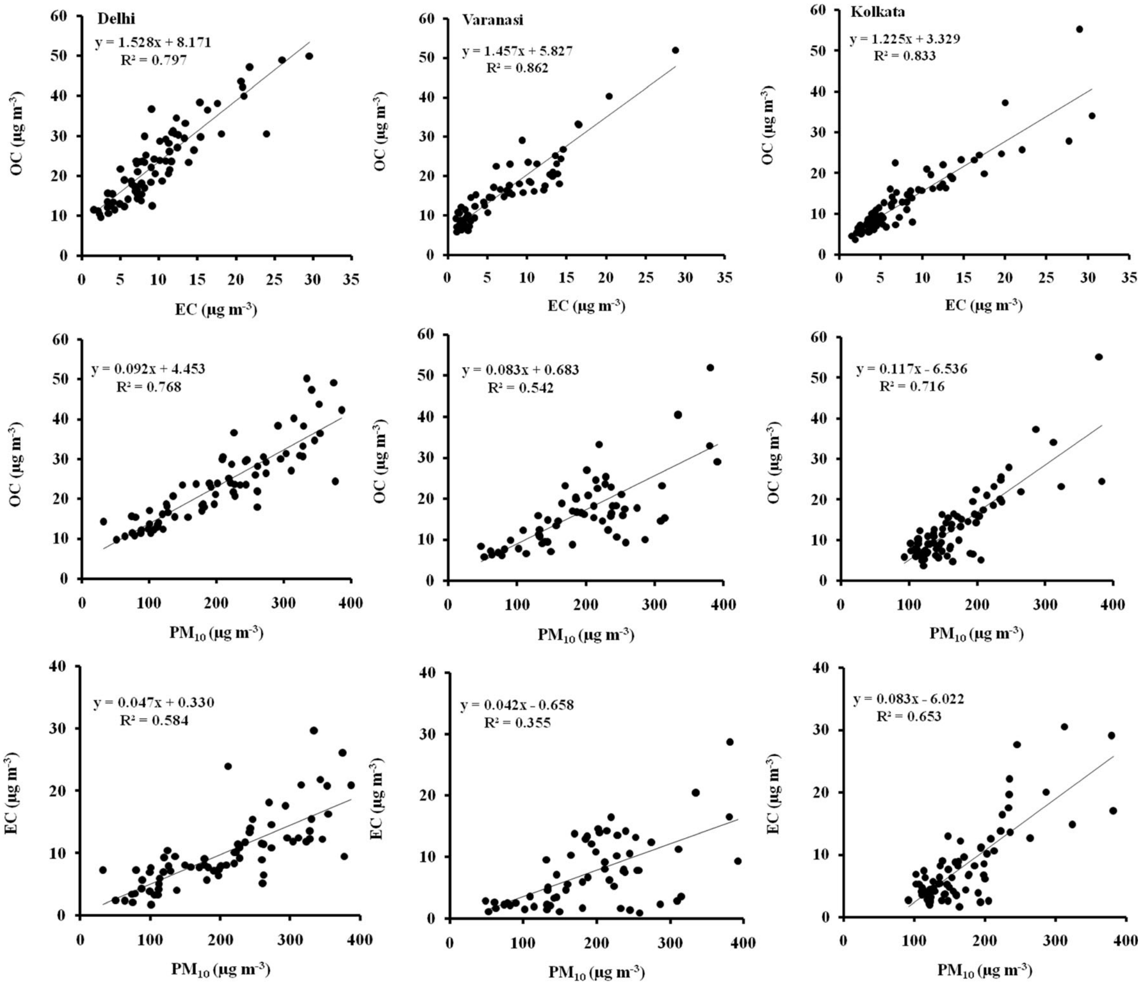

Fig. 5 Scatter plots between OC and EC, OC and PM_{10}, and EC and PM_{10} at Delhi, Varanasi, and Kolkata of IGP, India, during 2011

Kolkata (20.2 μg m^{-3}), whereas Varanasi has recorded the highest value (19.1 μg m^{-3}) in the month of February.

Water-soluble inorganic ionic components

The annual average and seasonal variation in concentrations of WSIC are summarized in Table 1 with seasonal difference over Delhi, Varanasi, and Kolkata of IGP, India. Over Delhi, among WSIC, SO_4^{2-} (11.6 μg m^{-3}) reports the highest concentration followed by other ionic compositions, e.g., NO_3^- (10.5 μg m^{-3}) > NH_4^+ (5.1 μg m^{-3}) > Cl^- (4.5 μg m^{-3}). Although Varanasi has encountered SO_4^{2-} (10.7 μg m^{-3}) as major component among WSIC, Kolkata has recorded SO_4^{2-} (10.0 μg m^{-3}) as a major component, followed by Cl^-, NO_3^-, NH_4^+, and Na^+ etc., (Table 1). The presence of Cl^- and SO_4^{2-} as a major ionic component over Kolkata may be due to the coastal region (Kolkata situated near the Bay of Bengal).

The monthly average variation in WSIC of PM_{10} mass over IGP, India, during 2011 is shown in Fig. 4. In the present study, the WSIC accounted for ~21, ~19, and ~24 % of PM_{10} mass at Delhi, Varanasi, and Kolkata, respectively, of IGI, India. Sharma et al. (2014b) reported the significant seasonal variation in concentration of particulate SO_4^{2-}, NO_3^-, and NH_4^+ over Delhi. The assimilation of HNO_3 into NH_4^+ aerosols generally depends on the amount of H_2SO_4 used in the neutralization with NH_3 (Sharma et al. 2012, 2014b). Thus, the samples containing lower SO_4^{2-} and higher NO_3^- concentration could be representative of local biogenic NO_x emission leading to formation of NO_3^- or marine masses having high Cl^- concentrations whereas the sample containing higher SO_4^{2-} and lower NO_3^- concentration could be representative of aerosols transported over a long distance or precursors from a continental air mass.

The result reveals that the molar ratio of NH_4^+ positively correlated with SO_4^{2-} and NO_3^- at Delhi Varanasi and Kolkata during winter (Figs. S5, S6, and S7; in supplementary information). However, molar ratio of NH_4^+ shows nonsignificant positive correlation with molar ratio of SO_4^{2-} and NO_3^- during monsoon at all locations. The assimilation of HNO_3 into NH_4^+ aerosols generally depends on the amount of H_2SO_4 used in neutralization with NH_3. Thus, the samples containing lower SO_4^{2-} and higher NO_3^- concentration could be representative of local biogenic NO_x emission leading to formation of NO_3^- or marine masses having high Cl^- concentrations whereas the sample containing higher SO_4^{2-} and lower NO_3^- concentration could be representative of aerosols transported over a long distance or precursors from a continental air mass, whereas NH_4^+ generally combines with NO_3^- and SO_4^{2-} in atmosphere and forms NH_4NO_3 and $(NH_4)_2SO_4$, respectively (Utsunomiya and Wakamatsu 1996; Behera and Sharma 2010). In $(NH_4)_2SO_4$, the molar ratio of NH_4^+ to SO_4^{2-} is 2:1. If the observed molar ratio is greater than 2, it signifies that excess NH_4^+ is present and possible may be combined with NO_3^- or other ions. In the present study, the equivalent molar ratio of NH_4^+/SO_4^{2-} computed as 2.73, 2.08, and 3.96 at Delhi, Varanasi, and Kolkata, respectively, which indicate the complete neutralization of atmospheric acid gas H_2SO_4 and predominant to aerosol formation during the study period. Similarly, the equivalent molar ratio of NH_4^+/NO_3^- i.e., 1.95 (Delhi), 1.54 (Varanasi), and 2.62 (Kolkata) indicate the formation of NH_4NO_3.

During the study period, SO_4^{2-} and NO_3^- ions also show the significant correlation with NH_4^+ indicating formation of $(NH_4)_2SO_4$ and NH_4NO_3 salt (Sharma et al. 2012a, b). The remainder of HNO_3 (after neutralization with NH_3) and/or H_2SO_4 may react with mineral dust to form $Ca(NO_3)_2$ and/or $CaSO_4$ in the coarse mode (Kholder and Hassan 2008; Guo et al. 2010; Rastogi and Sarin 2006). Significant correlation of NO_3^- with Ca^{2+} in PM_{10} samples indicates the possible association of NO_3^- with Ca^{2+} in the coarse mode. Thus, particulate-NH_4^+ is the major neutralizing agent of the acidic species (SO_4^{2-} and NO_3^-) in PM_{10}, whereas Ca^{2+} plays an important role in the neutralizing of the acidic species in the coarse mode aerosol over IGP (Ram and Sarin 2010).

Source apportionment

Figure 5 shows the scatter plot between OC and EC at Delhi ($R^2 = 0.797$; at $P < 0.05$), Varanasi ($R^2 = 0.862$; at $P < 0.05$), and Kolkata ($R^2 = 0.833$; at $P < 0.05$) during the study period (January–December 2011), whereas Figs. S2, S3, and S4 (in supplementary information) depicted on seasonality. A significant correlation between OC and EC is usually indicative of their common sources like vehicular traffic (Salma et al. 2004). In contrast, a poor correlation between OC and EC indicates the formation of secondary aerosol under favorable conditions for the gas to particle conversion of VOCs through a photochemical reaction in the atmosphere. Overall, a positive linear trend ($R^2 = 0.797$ for Delhi; $R^2 = 0.862$ for Varanasi; $R^2 = 0.833$ for Kolkata) is observed between OC and EC for at urban sites especially when OC concentrations are >50 μg m^{-3}, and it indicates the influence of vehicular emission (Salma et al. 2004). The scatter plots between OC and EC shows that during winter, summer, and monsoon over Delhi, Varanasi, and Kolkata of IGP, India, are significantly correlated and indicated the common sources of OC and EC over the region (Figs. :2, S3, and S4; in supplementary information).

In the present study, the annual ratio of OC/EC, K^+/OC, K^+/EC, Cl^-/EC, and SO_4^{2-}/EC of PM_{10} mass is recorded as 2.61, 0.08, 0.19, 0.47, and 1.15, respectively, over Delhi, whereas it was 1.75, 0.21, 0.35, 1.10, and 1.10, respectively, over Kolkata. Average values of K^+/EC and Cl^-/EC ratios are 0.19 and 0.47, respectively, over Delhi, which may give indication of presence of the biomass burning as well as fossil fuel combustion as a source of the PM_{10} mass at the observational site of Delhi (Yamasoe et al. 2000; Ferek et al. 1998; Saud et al. 2012).

The average OC/EC ratios of the present study over Delhi (2.61), Varanasi (2.31), and Kolkata (1.75) are relatively lower than those reported for the urban locations in China (Cao et al. 2003; Ho et al. 2007) and matches with earlier observations at few urban locations of the IGP (Table S1; in supplementary information). Such difference in the OC/EC ratio might depend on the differences in emission sources of carbonaceous aerosols (Ram and Sarin 2011; Sharma et al. 2014c). The OC and EC concentrations in present study sites might be attributed to the combined effects of traffic emission, biomass burning, wood burning, and crop residue burning. Analysis of stable carbon and nitrogen isotopic composition of PM_{10} mass indicated that the vehicular emissions, biomass burning, and secondary aerosols are the major source of PM_{10} mass over IGP, India (Sharma et al. 2015). Figure 5 shows the scatter plot between OC and EC during the study period for Delhi ($R^2 = 0.797$), Varanasi ($R^2 = 0.862$), and Kolkata ($R^2 = 0.833$). Ram and Sarin (2011) reported a significant linear relation between OC and EC ($r^2 = 0.66$) and OC and K^+ ($r^2 = 0.59$) of PM_{10} at Kanpur, IGP of India and attributed to biomass burning emissions which is one of the sources of PM_{10} over IGP India. A significant correlation between OC and EC is usually indicative of their common sources like vehicular traffic, biomass burning, etc. (Salma et al. 2004, Sharma et al. 2014c). Potassium (K) is generally used as a tracer of crustal dust in the coarse range and soluble K^+ for biomass burning in the fine range of PM (Sharma et al. 2014a). Soluble K^+ has been used as a key elemental marker for biomass/wood combustion for TSP, PM_{10}, and $PM_{2.5}$ (Khare and Baruah 2010; Shridhar et al. 2010). K^+ and NH_4^+ have also been used as markers for wood burning and agricultural activities (Khare and Baruah 2010). Fossil fuels could be the dominant sources of OC and EC in mega-cities like Delhi and Kolkata. Comparison of OC/EC, K^+/OC, K^+/EC, Cl^-/EC, and SO_4^{2-}/EC ratios in the particulates with present study and at different sites in India and China along with ratios for Savanna burning and agricultural waste burning are summarized in Table S1 (in supplementary information). In the above section, we have seen that variation of PM_{10} and their chemical composition (OC, EC, and WSIC) over three IGP regions, indicating the role of several sources. PCA and trajectory analysis may support and consolidate the idea depicted in the above section.

PCA was performed by the Varimax-rotated factor matrix method of SPSS for factor analysis on PM_{10} constituents collected over Delhi, Varanasi, and Kolkata of IGP, India. Eleven constituents of PM_{10} (OC, EC, Na^+, K^+, NH_4^+, Ca^{2+}, Mg^{2+}, F^-, Cl^-, NO_3^-, SO_4^{2}) were used as variables in the dataset at Delhi. Total 11 components were obtained, out of which three were extracted as principle components (Eigenvalue >1) that explained the 76 % of the variance of the data at Delhi. Three components corresponds to the different sources that were identified as secondary aerosol, biomass burning, fossil fuel combustion + vehicular emission, based on the loading of the

Table 2 PCA factor loadings for PM_{10} collected over Delhi, Varanasi, and Kolkata of IGP, India

	Delhi			Varanasi			Kolkata			
PM_{10}	Factor 1	Factor 2	Factor 3	Factor 1	Factor 2	Factor 3	Factor 1	Factor 2	Factor 3	Factor 4
OC	0.160	0.833	0.409	0.899	0.451	0.255	–	0.887	0.344	0.184
EC	0.124	0.613	0.817	0.867	0.764	0.364	–	0.930	0.150	0.161
F^-	–	–	0.121	–	–	–	0.563	–	–	0.143
Cl^-	0.372	0.726	0.222	–	0.934	–	0.888	0.191	0.199	–
SO_4^{2-}	0.694	0.162	0.409	0.078	0.028	0.880	0.199	0.077	0.814	–
NO_3^-	0.891	0.098	–	0.402	0.332	0.697	–	–	0.961	0.332
NH_4^+	0.849	0.098	0.047	0.651	–	0.643	0.321	0.612	0.501	–
Na^+	0.624	0.252	0.151	–	0.924	0.424	0.931	0.066	0.876	0.225
K^+	0.118	0.752	0.378	0.680	0.521	0.148	0.185	0.931	0.181	0.342
Mg^{2+}	0.441	0.201	0.640	0.476	0.716	0.294	0.112	0.206	0.641	0.155
Ca^{2+}	0.837	0.159	0.704	0.163	0.718	0.238	0.343	0.155	0.432	0.646
Eigenvalues	4.525	2.620	1.047	4.480	3.176	1.300	4.093	2.331	1.627	1.027
Variance (%)	41.139	23.818	9.522	40.726	28.872	11.821	37.209	21.187	14.790	9.339
Cumulative (%)	41.139	64.956	74.479	40.726	69.598	81.419	37.209	58.395	73.185	82.524
Source	Secondary aerosol	Biomass burning	Fossil fuel combustion + vehicular emission	Biomass burning	Vehicular emission + sea salt	Secondary aerosol	Sea salt	Biomass burning + vehicular emission	Secondary aerosol	Soil dust

Extraction method: principal component analysis; rotation method: Varimax with Kaiser Normalization; Eigenvalue >1.00; factor loading ≥0.30

variables in the factor (Table 2). The first factor is responsible for 41.14 % of the variance and high loading NH_4^+, NO_3^-, and SO_4^{2-} attributed to secondary aerosol whereas second factor attributed to biomass burning sources (OC, EC, and K^+). The third component indicated the combination of fossil fuel combustion + vehicular emission (~9.5 % of the total variance) exhibits high loading of EC, OC, and other metals.

PCA analysis also demonstrated the three factors to the different sources that were identified as secondary aerosol, biomass burning, vehicular emission + sea salt, and secondary aerosol based on the loading of the variables in the factor (Table 2) at Varanasi. The first factor is resolved 40.75 % of the variance and high loading OC, EC, and K^+ attributed to biomass burning whereas second factor attributed to vehicular emission + sea salt (EC, OC, K^+, Cl^-, Na^+, Mg^{2+}). The third factor attributed to secondary aerosol due high loading of NH_4^+, NO_3^-, and SO_4^{2-} in PM_{10} mass over Varanasi (Table 2).

The total 11 components were obtained, out of which four factors were extracted (with 82.5 % of the variance of the data) of PM_{10} mass at Kolkata. The four factors were identified as sea salt, biomass burning + vehicular emission, secondary aerosol, and soil dust based on the loading of the variables in the factor (Table 2). The first factor have high loading of Na^+ and Cl^- attributed to sea salt aerosol (~37 % of the total variance). The second factor attributed to biomass burning + vehicular emission (OC, EC, and K^+) whereas third component indicated secondary aerosol (Table 2).

Sharma et al. (2014a) reported soil dust (22.4 %), vehicle emissions (16.0 %), secondary aerosols (20.3 %), fossil fuel burning (16.6 %), biomass burning (11.8 %), industrial

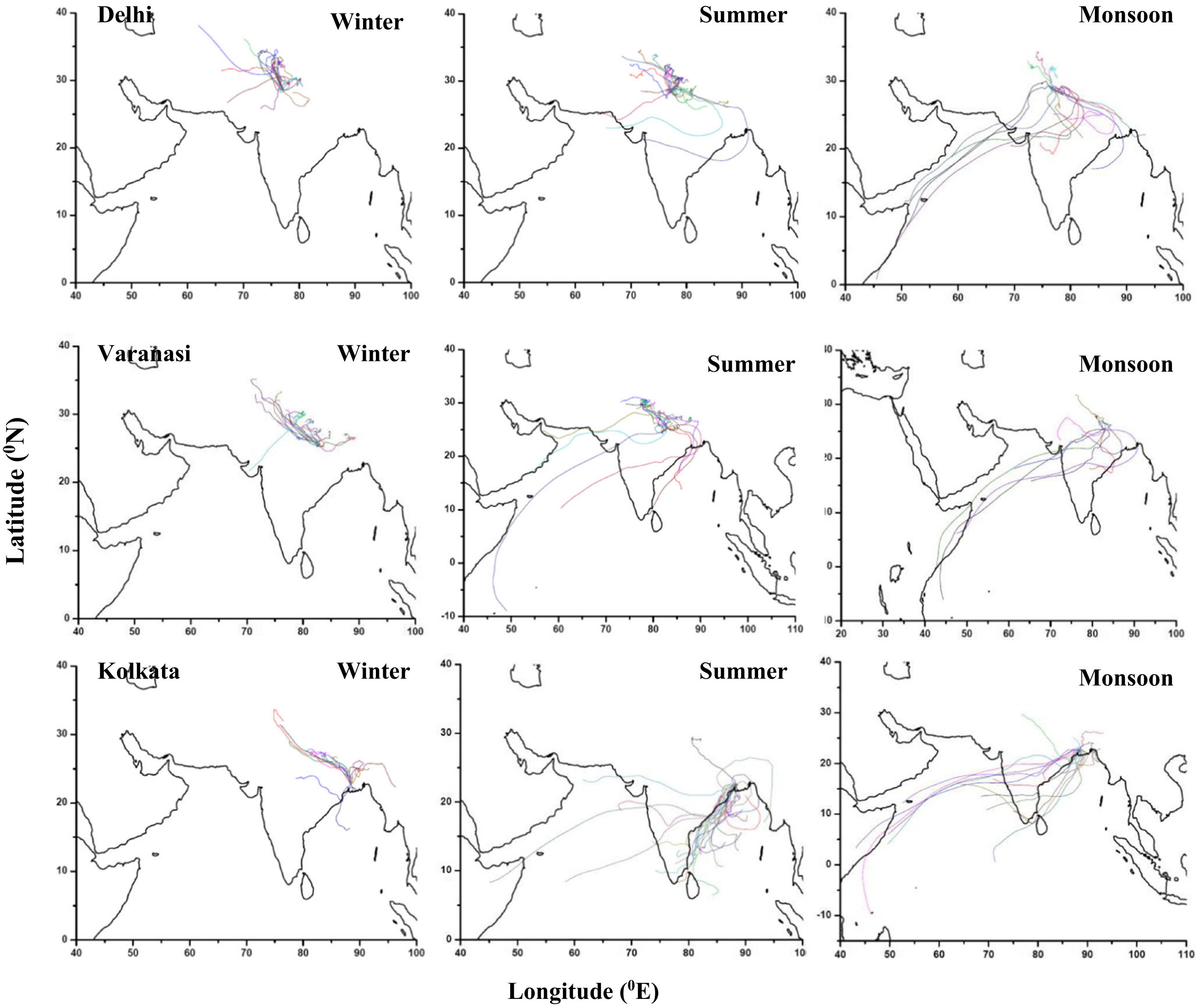

Fig. 6 Air parcel back trajectory (using HYSPLIT) during winter, summer, and monsoon period (GDAS meteorological data) over Delhi, Varanasi, and Kolkata of IGP, India

emissions (7.2 %), and sea salts (5.6 %) as the major sources of PM_{10} mass concentration at the observational site of Delhi using positive matrix factorization (PMF). Tiwari et al. (2009) reported that soil dust contributed 27.0 % of PM_{10} mass in Delhi whereas Khillare et al. (2004) estimated as 22.0 % soil dust of coarse particle at Delhi. Chelani et al. (2008) reported that soil dust and vehicular emission contributed 17.7 and 23.0 % of PM_{10} mass, respectively, at Mumbai whereas soil dust contributed 37.0 % of PM_{10} mass at Kolkata (Gupta et al. 2007).

In the above sections, we have observed the possible combined effect of biomass burning and fossil fuel combustion in the mass concentration of PM_{10} mass over three locations of IGP, India. However, the combined effect of biomass and fossil fuel largely depends on the local as well outflow of the long-distance source region. HYSPLIT has allowed for understanding the role of air mass parcel from long range transport at the receptor sites (Fig. 6). The approaching air mass at the receptor sites Delhi, Varanasi, and Kolkata during winter, summer, and monsoon seasons are depicted in Fig. 6. The approaching air mass at the receptor site Delhi is mainly continental type, being transported from IGP and its surroundings during winter and summer whereas air mass transported mainly from IGP and Arabian Sea through Thar Desert during monsoon (Sharma et al. 2014c). The approaching air mass at the receptor site of Varanasi is mainly from Punjab, Haryana, and Uttar Pradesh of IGP and surrounding areas during winter and summer whereas during monsoon, air mass parcel approaching mainly from Arabian Sea. At Kolkata the air mass is approaching the observational site from the IGP and surrounding areas during winter season. During summer and monsoon, air mass is approaching at the observational site of Kolkata mainly from coastal areas of the Bay of Bengal and Arabian Sea, respectively.

Conclusions

Source apportionment of simultaneously observed PM_{10} at three locations, viz., Delhi (upper IGP), Varanasi (middle IGP), and Kolkata (lower IGP) and its chemical properties (OC, EC, and WSIC) for the year 2011 provide following points:

- During study period, higher average mass concentration of PM_{10} at Varanasi (206.2 $\mu g\ m^{-3}$) followed by Delhi (202.3 $\mu g\ m^{-3}$) and Kolkata (171.5 $\mu g\ m^{-3}$) indicates combination of the growth of fine particulates on the way from upper IGP region, local sources (transport for usage of adulterated oil, brick kiln, biomass burning, etc.).
- The higher average PM_{10} mass during winter are either due to capping by low-level boundary layer increasing the average burden (Delhi and Varanasi) or due to the movement of ITCZ when low-level northeast wind flow carries large amount of pollutants along with (Kolkata). Particulate matter has been washed out during heavy rain over three locations during monsoon. Over Kolkata, large marine sources (sea salt) might have increased the concentration of PM_{10} during monsoon.
- It has been noticed that concentration of OC, EC, and TC has followed the pattern of variation of PM_{10} mass concentration with maximum concentration broadly in winter (December–February) over the three stations. The maximum average concentration of OC has been recorded at Delhi (23.57 $\mu g\ m^{-3}$) and minimum at Kolkata (12.74 $\mu g\ m^{-3}$).
- OC/EC, K^+/OC, K^+/EC, Cl^-/EC, and SO_4^{2-}/EC ratios of PM_{10} indicate the role of different sources over three IGP regions. The average OC/EC ratios of the present study over Delhi (2.61), Varanasi (2.31), and Kolkata (1.75) are relatively lower than those reported for the urban locations in China and matches with earlier observations at few urban locations of the IGP
- The positive linear relationship of molar ratios of SO_4^{2-} and NO_3^- with NH_4^+ indicates the possibility of the formation of secondary inorganic aerosol [$(NH_4)_2SO_4$ and NH_4NO_3] over IGP region. Air mass flow at the observational sites indicate the continental and marine types PM_{10} transported from the Bay of Bengal, Pakistan, Thar Desert, IGP region and surrounding areas.
- PCA analysis of PM_{10} quantifies that secondary aerosol, biomass burning, vehicular emission, and fossil fuel combustion are the major sources of PM_{10} at Delhi whereas biomass burning, secondary aerosol, vehicular emission, and sea salt are the major sources at Varanasi. At Kolkata, the major sources of PM_{10} mass resolve as sea salt, secondary aerosol, biomass burning, vehicular emission, and soil dust.

Acknowledgments The authors are thankful to the Director, CSIR-NPL, New Delhi, and Head Radio and Atmospheric Sciences Division, CSIR-NPL, New Delhi, for their encouragement and support for this study. The authors also acknowledge Council of Scientific and Industrial Research (CSIR), New Delhi, for providing financial support for this study (under CSIR-EMPOWER Project: OLP-102132). Authors are thankful to the anonymous reviewers for their constructive suggestions to improve the manuscript.

References

Behera SN, Sharma N (2010) Investigating the potential role of ammonia in ion chemistry of fine particulate matter formation for an urban environment. Sci Total Environ 408:3569–3575

Bond TC, Doherty SJ, Fahey DW et al (2013) Bounding the role of black carbon in the climate system: a scientific assessment. J Geophys Res Atmos 118:5380–5552

Chelani AB, Gajghate DG, Devotta S (2008) Source apportionment of PM10 in Mumbai, India using CMB model. Bull Environ Contam Toxicol 81:190–195

Chow JC, Watson JG, Chen LWA, Arnott WP, Moosmuller H (2004) Equivalence of elemental carbon by thermal/optical reflectance and transmittance with different temperature protocols. Environ Sci Technol 38:4414–4422

Cao JJ, Lee SC, Ho KF, Zhang XY, Zou SC, Fung K, Chow JC, Watson JG (2003) Characteristics of carbonaceous aerosol in Pearl River Delta region, China during 2001 winter period. Atmos Environ 37: 1451–1460

Das M, Maiti SK, Mukhopadhyay U (2006) Distribution of PM2.5 and p M10–2.5 in PM10 fraction in ambient air due to vehicular pollution in Kolkata megacity. Environ Monit Assess 122(1–3):111–123

Datta A, Saud T, Goel A, Tiwari S, Sharma SK, Saxena M, Mandal TK (2010) Variation of ambient SO_2 over Delhi. J Atmos Chem 65(2–3):127–143

Delhi Statistical Handbook (2012) Registered vehicles in Delhi. Directorate of Economics and Statistics. Govt. of National Capital, Delhi. www.des.delhigovt.nic.in

Draxler, R. R., Rolph, G. D. (2003) HYSPLIT (HYbrid Single-Particle Lagrangian Integrated Trajectory) Model access via NOAA ARL READY Website (http://www.arl.noaa.gov/ready/hysplit4.html). NOAA Air Resources Laboratory, Silver Spring, MD

Ferek RJ, Reid JS, Hobbs PV (1998) Emission factors of hydrocarbons, halocarbons, trace gases and particles from biomass burning in Brazil. J Geophys Res 103(D24):32107–32118

Goyal P, Sidhartha (2002) Effect of winds on SO_2 and SPM concentration in Delhi. Atmos Environ 36:2925–2930

Guinot B, Cachier H, Sciare J, Tong Y, Xin W, Jianhua Y (2007) Beijing aerosol: atmospheric interactions and new trends. J Geophys Res 112:D14314. doi:10.1029/2006JD008195

Guo S, Hu M, Wang ZB, Slanina J, Zhao YL (2010) Size-resolved aerosol water soluble Ioninc compositions in the summer of Beijing: implication of regional secondary formation. Atmos Chem Phys 10:947–959

Gupta AK, Karar K, Srivastava A (2007) Chemical mass balance source apportionment of PM10 and TSP in residential and industrial sites of an urban region of Kolkata, India. J Hazard Mater 142:279–287

Ho KF, Cao JJ, Lee SC, Kawamura K, Zhang R-J (2007) Dicarboxylic acids, ketocarboxylic acids and dicarbonyls in urban atmosphere of China. J Geophys Res 112:D22S27. doi:10.1029/2006JD008011

Jacobson MZ (2001) Strong radiative heating due to the mixing state of black carbon in atmospheric aerosols. Nature 409:695–697

Khare P, Baruah BP (2010) Elemental characterization and source identification of $PM_{2.5}$ using multivariate analysis at the suburban site of North-East India. Atmos Res 98:148–162

Khillare PK, Balachandran S, Meena BR (2004) Spatial and temporal variation of heavy metals in atmospheric aerosol in India. Environ Monit Assess 90:1–21

Kholder MI, Hassan SK (2008) Weekday/weekend differences in ambient aerosol level and chemical characteristics of water soluble components in the city Centre. Atmos Environ 42:7483–7493

Li X, Wang S, Duan L, Hao J, Nie Y (2009) Carbonaceous aerosol emissions from household biofuel combustion in China. Environ Sci Technol 43:6076–6081

Liousse C, Penner JE, Chuang C, Walton JJ, Eddleman H, Cachier H (1996) A global three-dimensional model study of carbonaceous aerosol. J Geophys Res 101:19411–19432

Mandal P, Saud T, Sarkar R, Mandal A, Sharma SK, Mandal TK, Bassin JK (2014) High seasonal variation of atmospheric C and particulate concentrations in Delhi, India. Environ Chem Letts 12:225–230

Murari V, Kumar M, Barman SC, Banerjee T (2014) Temporal variability of MODIS aerosol optical depth and chemical characterization of airborne particulates in Varanasi, India. Environ Sci Pollut Res doi. doi:10.1007/s11356-014-3418-2

Pandey P, Patel DK, Khan AH, Barman SC, Murthy RC, Kisku GC (2013) Temporal distribution of fine particulates (PM2.5, PM10), potentially toxic metals, PAHs and Metal-bound carcinogenic risk in the population of Lucknow City, India. J Environ Sci Health 48(7):730–745

Perrino C, Tiwari S, Catrambone M, Torre SD, Rantica E, Canepari S (2011) Chemical characterization of atmospheric PM in Delhi, India during different periods of the year including Diwali festival. Atmos Pollut Res 2:418–427

Pope CA, Dockery DW (2006) Health effects of fine particulate air pollution: lines that connect. JAPCA 56:709–742

Pope CA, Ezzati M, Dockery DW (2009) Fine-particulate air pollution and life expectancy in the United States. New Engl J Med 360:376–386

Ram K, Sarin MM (2010) Spatio-temporal variability in atmospheric abundances of EC, OC and WSOC over northern India. J Aerosol Sci 41(1):88–98

Ram K, Sarin MM (2011) Day–night variability of EC, OC, WSOC and inorganic ions in urban environment of Indo-Gangetic Plain: implications to secondary aerosol formation. Atmos Environ 45:460–468

Ram K, Sarin MM, Tripathi SN (2010) One-year record of carbonaceous aerosols from an urban location (Kanpur) in the Indo-Gangetic Plain: characterization, sources and temporal variability. J Geophys Res. doi:10.1029/2010JD014188

Ram K, Sarin MM, Sudheer AK, Rengarajan R (2012) Carbonaceous and secondary aerosols during wintertime fog and haze over urban sites in the Indo-Gangetic Plain. Aero Air Qual Res 12:359–370

Ramgolam K, Favez O, Cachier H, Gaudichet A, Marano F et al (2009) Size-partitioning of an urban aerosol to identify particle determinants involved in the proinflammatory response induced in airway epithelial cells. Part Fibre Toxicol 6:1–12

Rastogi N, Sarin MM (2006) Chemistry of aerosols over a semi arid region: evidence for acid neutralization by mineral dust. Geophys Res Lett 33:L23815. doi:10.1029/2006 GL027708

Salma I, Chi XG, Maenhaut W (2004) Elemental and organic carbon in urban canyon and background environments in Budapest, Hungary. Atmos Environ 38:2517–2528

Saud T, Singh DP, Mandal TK, Gadi R, Pathak H, Saxena M, Sharma SK, Gautam R, Mukherjee A, Bhatnagar RP (2011) Spatial distribution of biomass consumption as energy in rural areas of Indo-Gangetic plain. Biomass Bioenergy 35:932–941

Saud T, Gautam R, Mandal TK, Gadi R, Singh DP, Sharma SK, Dahiya M, Saxena M (2012) Emission estimates of organic and elemental carbon from household biomass fuel used over the Indo-Gangetic Plain (IGP), India. Atmos Environ 61:212–220

Saud T, Saxena M, Singh DP, Saraswati, Dahiya M, Sharma SK, Datta A, Gadi R, Mandal TK (2013) Spatial variation of chemical constituents of commonly used biomass fuels in rural areas of the Indo-Gangetic Plain (IGP), India. Atmos Environ 71:158–169

Schwartz J, Dockery DW, Neas LM (1996) Is daily mortality associated specifically with fine particle? J Air Pollut Control Assess 46:927–939

Sen A, Ahammed YN, Banerjee T, Begam GR, Burah BP, Chatterjee A, Choudhuri AK, Dhir A, Das T, Dhayni PP, Deb NC, Gadi R, Ghosh S, Gupta A, Sharma KC, Khan AH, Kumari KM, Kumar M, Kuniyal JC, Lakhani A, Meena RK, Mahapatra PS, Naqvi SWA, Pal D, Pal S, Panda S, Rohtash, Saikia J, Saikia P, Sharma A, Sharma P, Saxena M, Shenoy DM, Vachaspati CV, Sharma SK, Mandal TK (2014) Atmospheric fine and coarse mode aerosols at different environments of India and the Bay of Bengal during winter-2014: implication of a coordinated campaign. Mapan-J Metro Soc India 29(4):273–284

Sharma M, McBean EA, Ghosh U (1995) Prediction of atmospheric sulphate deposition at sensitive receptors in northern India. Atmos Environ 29:2157–2162

Sharma M, Kishore S, Tripathi SN, Behra SN (2007) Role of atmospheric ammonia in the formation of inorganic secondary particulate matter: a study at Kanpur, India. J Atmos Chem 58:1–17

Sharma SK, Datta A, Saud T, Mandal TK, Ahammed YN, Arya BC, Tiwari MK (2010) Study on concentration of ambient NH3 and interaction with some other ambient trace gases. Environ Monit Assess 162:225–235

Sharma SK, Singh AK, Saud T, Mandal TK, Saxena M, Singh S, Ghosh S, Raha S (2012a) Study on water soluble ionic composition of PM_{10} and trace gases over Bay of Bengal during W_ICARB campaign. Meteorog Atmos Phys 118:37–51

Sharma SK, Saxena M, Saud T, Korpole S, Mandal TK (2012b) Measurement of NH_3, NO, NO_2 and related particulates at urban sites of Indo Gangetic Plain (IGP) of India. J Sci Ind Res 71(5):360–362

Sharma SK, Mandal TK, Saxena M, Rashmi, Rohtash, Sharma A, Gautam R (2014c) Source apportionment of PM_{10} by using positive matrix factorization at an urban site of Delhi, India. Urban Climate 10(4):656–670

Sharma SK, Kumar M, Rohtash, Gupta NC, Saraswati, Saxena M, Mandal TK (2014b) Characteristics of ambient ammonia over Delhi, India. Meteorog Atmos Phys 124:225–230

Sharma SK, Mandal TK, Saxena M, Rashmi, Datta A, Saud T (2014a) Variation of OC, EC, WSIC and trace metals of PM_{10} over Delhi. J Atmos Sol Terr Phys 113:10–22

Sharma SK, Mandal TK, Sharma C, Kuniyal JC, Joshi R, Dhayani PP, Rohtash, Sen A, Ghayas H, Gupta NC, Arya BC, Kumar A, Sharma P, Saxena M, Sharma A (2014d) Measurements of particulate ($PM_{2.5}$), BC and trace gases over the northwestern Himalayan region of India. Mapan - J Meteorol Soc India 29(4):243–253

Sharma SK, Mandal TK, Shenoy DM, Bardhan P, Srivastava MK, Chatterjee A, Saxena M, Saraswati, Singh BP, Ghosh SK (2015) Variation of stable carbon and nitrogen isotopes composition of PM_{10} over Indo Gangetic Plain of India. Bull Environ Contam Toxicol 95(5):661–669

Shridhar V, Khillare PS, Agarwal T, Ray S (2010) Metallic species in ambient particulate matter at rural and urban location of Delhi. J Hazard Mater 175:600–607

Song Y, Zhang Y, Xie S, Zeng L, Zheng M, Salmon LG, Shao M, Slanina S (2006) Source apportionment of PM2.5 in Beijing by positive matrix factorization. Atmos Environ 40(1):526–1537

Tare V, Tripathi SN, Chinnam N, Srivastava AK, Dey S, Manar M, Kanawade VP, Aggarwal A, Kishore L, Lal RB, Sharma M (2006) Measurement of atmospheric parameters during Indian space research organization geosphere biosphere program land campaign II at a typical location in the Ganga Basin: 2 chemical properties. J Geophys Res 111:D23210. doi:10.1029/2006/JD007279

Tiwari S, Srivastava AK, Bisht DS, Bano T, Singh S, Behura S, Srivastava MK, Chate DM, Padmanabhamurthy B (2009) Black carbon and chemical characteristics of PM_{10} and $PM_{2.5}$ at an urban site of North India. J Atmos Chem 62:193–209

Tiwari S, Chate DM, Pragya P, Ali K, Bisht DS (2012) Variations in Mass of the PM10, PM2.5 and PM1 during the Monsoon and the Winter at New Delhi. Aerosol Air Qual Res 12(1):20–29

Utsunomiya A, Wakamastsu S (1996) Temperature and humidity dependence on aerosol composition in the northern Kyushu. Jpn Atmos Environ 30:2379–2386

Waked A, Favez O, Alleman LY, Piot C, Petit JE, Delaunay T et al (2014) Source apportionment of PM10 in a north-western Europe regional urban backgroung site (Lens, France) using positive matrix factorization and including primary biogenic emission. Atmos Chem Phys 14:3325–3346

Yamasoe MA, Artaxo P, Miguel AH, Allen AG (2000) Chemical composition of aerosol particles from direct emissions of vegetation fires in the Amazon Basin: water-soluble species and trace elements. Atmos Environ 34:1641–1653